

Eco-Friendly Hydrothermal Synthesis and Characterization of Cobalt Ferrite Nanoparticles without Post-Processing

Soumen Mondal¹, Dr. Devendra Pradhan²

^{1,2}Department of Physics, Mansarovar Global University, Sehore, M.P., India.

ABSTRACT

Cobalt ferrite (CoFe₂O₄) nanoparticles were synthesized via a green hydrothermal method using ethylene glycol as a solvent and Arabic gum as a natural stabilizer, without any post-processing steps. Ferric nitrate and cobalt nitrate were dissolved in ethylene glycol, followed by the dropwise addition of ammonia solution under controlled stirring and temperature conditions. The mixture was subjected to hydrothermal treatment at 180 °C for 4 hours. The obtained black precipitate was washed with water and ethanol and dried at 100 °C. A comparative non-hydrothermal sample was also prepared. Various synthesis parameters including reaction time, temperature, ethylene glycol concentration, pH, and Arabic gum amount were systematically varied to study their effect on particle formation.

X-ray diffraction confirmed the crystalline spinel structure of cobalt ferrite. FT-IR analysis revealed characteristic metal-oxygen vibrations. HR-TEM and SAED images showed well-defined nanoparticles with uniform morphology. FE-SEM and EDS analysis confirmed elemental composition and surface structure. UV-Vis diffuse reflectance spectroscopy showed strong absorption in the visible region, confirming the semiconducting nature of the material. The method offers an eco-friendly, simple, and efficient approach to synthesize cobalt ferrite nanoparticles with controlled morphology and crystallinity.

Keywords: Cobalt Ferrite, Nanoparticles, Hydrothermal, Ecofriendly, Characterization.

INTRODUCTION

Nanotechnology has emerged as a transformative scientific field over the past few decades, offering significant advancements in materials science, medicine, electronics, and energy applications. Among the various classes of nanomaterials, magnetic nanoparticles have drawn particular attention due to their unique physical and chemical properties, especially at the nanoscale. Within this group, spinel ferrites with the general formula MFe₂O₄ (where M represents a divalent metal ion such as Co, Ni, Mn, or Zn) have been extensively investigated. Cobalt ferrite (CoFe₂O₄), a well-known magnetic spinel ferrite, is distinguished by its high chemical stability, moderate saturation magnetization, large magnetocrystalline anisotropy, and mechanical hardness. These properties make cobalt ferrite an ideal candidate for diverse applications such as magnetic data storage, catalysis, biomedical imaging, drug delivery, and environmental remediation.

Despite its promising characteristics, the synthesis of cobalt ferrite nanoparticles poses challenges in terms of controlling size, morphology, and crystallinity. Traditional chemical synthesis methods, such as sol-gel, co-precipitation, and combustion, often involve high temperatures, toxic solvents, and multiple post-processing steps, which can be environmentally hazardous and economically inefficient. These conventional methods may also result in particle agglomeration, non-uniform shapes, and impurities, which adversely affect the final properties of the nanoparticles. As the global scientific community moves toward more sustainable practices, the development of eco-friendly and cost-effective synthetic approaches has become a priority.

In this context, hydrothermal synthesis presents itself as a viable green alternative. It involves the use of high-pressure and high-temperature aqueous conditions to facilitate the crystallization of materials in a controlled environment. This method allows for precise control over particle size, shape, and phase purity, often eliminating the need for post-synthesis treatments such as calcination or annealing. Moreover, the hydrothermal method typically operates at relatively lower temperatures compared to other thermal methods, making it energy-efficient. The closed-system nature of the autoclave setup also reduces the release of toxic byproducts, aligning well with principles of green chemistry.



To enhance the environmental friendliness of the hydrothermal method, the choice of solvents and stabilizers becomes crucial. Ethylene glycol (EG) is a widely used polyol that serves not only as a solvent but also as a reducing and stabilizing agent due to its high boiling point and viscosity. Its use in nanoparticle synthesis helps minimize particle agglomeration and supports the formation of uniform nanostructures. Additionally, the incorporation of natural biopolymers such as Arabic gum (AG) further enhances the eco-friendly nature of the synthesis. Arabic gum, a water-soluble natural polymer extracted from Acacia trees, acts as a non-toxic surfactant and stabilizer that prevents particle aggregation and promotes homogeneity during nanoparticle formation.

In this study, cobalt ferrite nanoparticles were synthesized using a green hydrothermal route that integrates ethylene glycol and Arabic gum, without requiring any further post-processing such as calcination. The synthesis was conducted by reacting cobalt and ferric nitrates in an ethylene glycol medium, followed by ammonia addition and hydrothermal treatment in a Teflon-lined autoclave at 180 °C. The synthesized nanoparticles were thoroughly washed and dried, avoiding any post-synthesis high-temperature treatment, thus preserving their eco-friendly nature. A non-hydrothermal sample was also prepared for comparison to understand the influence of hydrothermal conditions on the material properties.

Moreover, the effect of various reaction parameters on the structural and morphological properties of the synthesized cobalt ferrite nanoparticles was systematically investigated. These parameters included reaction time, hydrothermal temperature, ethylene glycol concentration, pH of the reaction mixture, and the amount of Arabic gum used. Fine-tuning these variables allowed for better control over the size, morphology, and crystalline quality of the nanoparticles, making it possible to tailor the material for specific applications.

The synthesized nanoparticles were characterized using a range of analytical techniques to confirm their structural, morphological, and optical properties. X-ray diffraction (XRD) was used to identify the crystal structure and phase purity. Fourier-transform infrared spectroscopy (FT-IR) provided information on chemical bonding and the presence of metal-oxygen functional groups. High-resolution transmission electron microscopy (HR-TEM) and selected area electron diffraction (SAED) offered insights into the nanoparticle morphology and crystallinity. Field emission scanning electron microscopy (FE-SEM) coupled with energy-dispersive X-ray spectroscopy (EDS) was employed to examine surface texture and elemental composition. Finally, UV-Vis diffuse reflectance spectroscopy was used to assess the optical behavior of the materials.

This work demonstrates that a simple, scalable, and environmentally benign hydrothermal process can be effectively employed for the synthesis of cobalt ferrite nanoparticles with desirable structural and functional characteristics. The method provides a promising route for the large-scale production of magnetic nanomaterials suitable for a variety of industrial and biomedical applications while adhering to the principles of green chemistry.

REVIEW OF LITERATURE

Weißpflog, Maria et al., (2024) Magnetic CoxFe3-xO4 nanoparticles (NPs, 0.2 < x < 0.5) were generated via a two-step synthesis of cigar-shaped akaganeite precursors and later conversion by hydrothermal reaction with varied molar ratios of Co2+/Fe2+/Fe3+ chloride salts. Both procedures were effectively done in aqueous medium without utilizing hazardous surfactants and solvents. To examine the influence of cobalt ion concentrations, magnetic and hyperthermia measurements were studied in reliance on the size, shape, and composition of the samples. The lowering of the cobalt level by up to 52% did not affect the hyperthermia readings significantly and provides a greener synthesis technique Tamboli, Qudsiya et al., (2023) Exploration and use of nanotechnology are booming across all industries. Numerous scientists have taken an interest in magnetic nanoparticles, especially nanoferrites, due to their expanding list of potential uses.

The most important and researched magnetic nanoparticle among them is nanocobalt ferrite. Minimizing environmental and occupational dangers necessitated the use of synthetic approaches that were gentler on the environment. In recent years, green synthesis methods have seen extensive use in the production of nanomaterials. Using a variety of scientific search engines, we surveyed current practices for creating nanocobalt ferrites and composites with these metals. Environmental (water/wastewater treatment, photocatalytic dye degradation, and nanosorbent for environmental remediation) and biomedical (nanobiosensors for early-stage cancer diagnosis, hyperthermia, hyperresonance imaging, targeted drug delivery, magnetic resonance imaging, and possible drug candidates against cancer and microbial infections) applications were subsequently covered. This article provides in-depth information on the advantages of green synthesis of nanocobalt ferrite as opposed to traditional techniques, as well as how to choose suitable natural resources for this process.

Coppola, Priscilla et al., (2016) we create magnetic nanoparticles of Zn-substituted cobalt ferrite (Znx Co1-x Fe2O4, with $0 \le x \le 1$) using a hydrothermal co-precipitation technique in an alkaline media. A combination of energy-dispersive X-ray spectroscopy and atomic absorption spectroscopy is used to determine the chemical composition. Transmission electron microscopy (TEM) and X-ray diffraction (XRD) are used to study the nanopaticles' shape and



structure, respectively. Clarifications using XRD Rietveld show how the cations are distributed across the A and B sites. The results demonstrate that zinc ions preferentially occupy A-sites up to x \sim 0.5, after which Zn ions also start to gradually occupy B-sites. Microscopy photos reveal nanoparticles in a variety of forms, including spherical, cubic, and octahedron. At 300 and 5 K, the hysteresis loop's characteristics are examined. The ratio of zinc to cobalt in the nanoparticles has a significant impact on these characteristics. Only samples with a large amount of Co exhibit hysteresis at 300 K. C

Zalite, Ilmars et al., (2015) the co-precipitation technique and hydrothermal synthesis method are used to create cobalt ferrite powders. The synthesized products are evaluated for magnetic characteristics, specific surface area (SSA), and crystallite size. With a crystallite size ranging from 10 to 16 nanometers, an SSA of 60 to 65 micrometers per gram, and a predicted particle size of 20 to 22 nanometers, all of the produced ferrites are single phase nanocrystalline materials. Coercivity Hc = 570-650 Oe, saturation magnetization MS = 59-60 emu/g, and remanent magnetization Mr = 23 emu/g are the characteristics of the Co ferrites that have been synthesized.

Koseoglu, Yuksel et al., (2012) A hydrothermal technique aided by polyethylene glycol was used to successfully manufacture a series of cobalt ferrite compounds doped with Mn, with the formula MnxCo1-xFe2O4 with values of x ranging from 0.0 to 1.0. The cubic spinel structure was seen in all of the samples. The nanoparticles' average crystallite sizes, as determined by Debye-Scherrer's equation, were determined to be 14–22 nm, with a very tiny size distribution. As predicted from the synthesis, the compositional mass ratios were crucial, and scanning electron microscopy (SEM) was employed to examine morphological changes.

EDX findings confirmed this. According to VSM measurements, there are two phases in every sample: ferromagnetic and superparamagnetic. The blocking temperatures between the phases drop as the Mn concentration increases. The same holds true for the samples' coercive fields and remanent magnetizations; they tend to diminish as x increases from 0.0 to 1.0. At temperatures below the blocking temperature, they exhibit ferromagnetic properties. As the temperature drops, the samples' magnetization and coercive field become stronger.

Goodarz naseri, Mahmoud et al., (2010) Aqueous solutions containing metal nitrates and polyvinyl pyrrolidone (PVP) were heated and then calcined at temperatures ranging from 673 to 923 K to produce crystalline, magnetic, cobalt ferrite nanoparticles. Transmission electron microscopy (TEM), Fourier transform infrared spectroscopy (FT-IR), and X-ray diffraction (XRD) were used to ascertain the structural properties of the calcined samples. The fact that the FT-IR spectra do not reveal any organic absorption bands indicates that crystallization was complete between 823 and 923 K. Vibrating sample magnetometer (VSM) tests conducted at room temperature demonstrated that the calcined samples had conventional magnetic characteristics.

EXPERIMENTAL DETAILS

Materials and reagents

In India, Sd Fine-Chem Limited (SDFCL) supplied ferric nitrate nonahydrate ($Fe(NO_3)_3 \cdot 9H_2O$) and ethylene glycol ($C_2H_6O_2$). Cobalt nitrate hexahydrate ($Co(NO_3)_2 \cdot 6H_2O$) was obtained from Alpha Chemika, India. Sodium hydroxide (NaOH) pellets, ethanol (C_2H_3OH , 70% v/v), and ammonia solution (NH_3 , 25% w/w) were procured from El-Nasr Pharmaceutical Chemicals Company (ADWIC), Egypt. Arabic gum (AG) was sourced from LOBA Chemie, India. All reagents were used as received, without further purification.

Preparation of cobalt ferrite nanoparticles

Nanoparticles of cobalt ferrite were produced using a hydrothermal process. Iron (III) nitrate nonahydrate (6.4 g, 15.84 mmol, 2 eq.) and cobalt (II) nitrate hexahydrate (2.305 g, 7.92 mmol, 1 eq.) were dissolved in 40 mL of ethylene glycol, respectively, before being combined with stirring. The solution was heated to 70 °C after production. A 3 M aqueous ammonia solution (50 mL) was added drop wise to the heated and swirling solution.

Then, the brown reaction mixture was moved to an autoclave lined with Teflon after being stirred for 30 minutes at 70 °C. Once sealed, the autoclave was put in an oven preheated to 180 °C for duration of 4 hours. Once the autoclave had cooled down to room temperature, the black precipitate was removed and rinsed with a mixture of bi-distilled water and 70% ethanol until the pH level of the wash water became neutral.

The electric oven was set to $100 \, ^{\circ}\text{C}$ for about 5 hours to dry the precipitate that had separated. A second sample was made under identical circumstances, with the exception of the hydrothermal treatment, so that we could compare the two. The created specimen was marked as CF. However, we looked at how different variables affected the hydrothermal experiment, including (a) reaction time (0.5, 4, and 8 h), (b) temperature (180, 150, and 120 $^{\circ}\text{C}$), (c) ethylene glycol concentration (100%, 75%, 50%, 25%, 0% (v/v)), (d) pH value (measured with an ammonia solution, 9.6, 9, and 8), and (e) AG proportion (0.5, 1, and 2 g). Table 1 lists the samples that were hydrothermally produced.



Proposed reaction mechanism of cobalt ferrite nanoparticles formation

$$Co(NO_{3})_{2}.6H_{2}O_{(s)} \xrightarrow{H_{2}O} [Co(H_{2}O)_{6}]^{2+}_{(aq)} + 2NO_{3}^{-}_{(aq)} (1)$$

$$Fe(NO_{3})_{3}.9H_{2}O_{(s)} \xrightarrow{H_{2}O} [Fe(H_{2}O)_{6}]^{3+}_{(aq)} + 3NO_{3}^{-}_{(aq)} + 3H_{2}O_{(2)}$$

$$[Co(H_{2}O)_{6}]^{2+}_{(aq)} \xrightarrow{NH_{4}OH} [Co(OH)_{x}]^{2-x}_{(aq)} \xrightarrow{NH_{4}OH} Co(OH)_{2}_{(s)} \xrightarrow{NH_{4}OH} [Co(OH)_{3}]^{-}_{(aq)} (3)$$

$$[Fe(H_{2}O)_{6}]^{3+}_{(aq)} \xrightarrow{NH_{4}OH} [Fe(OH)_{y}]^{3-y}_{(aq)} \xrightarrow{NH_{4}OH} Fe(OH)_{3}_{(s)} \xrightarrow{NH_{4}OH} [Fe(OH)_{4}]^{-}_{(aq)} (4)$$

$$[Co(OH)_{3}]^{-}_{(aq)} + [Fe(OH)_{4}]^{-}_{(aq)} \xrightarrow{hydrothermal conditions} CoFe_{2}O_{4}_{(s)} + 4H_{2}O_{(f)} + 3OH_{(aq)}^{-} (5)$$

Characterization of cobalt ferrite nanoparticles

The researchers from the Central Metallurgical R&D Institute used an X-ray powder diffractometer (Bruker Co. D8 Advanced) with a copper K α radiation source ($\lambda = 1.5406$ Å), a 40 kV generator voltage, and a 40 mA generator current to conduct the crystallographic examinations of cobalt ferrite (CoFe₂O₄) nanoparticles. A scanning rate of 0.02°/0.4 s was used to examine the powder sample throughout a 2 θ range of 10–80°. Fourier transform infrared (FT-IR) spectra were acquired using a Thermo Fisher Nicolet IS10 spectrometer. Room temperature FT-IR spectra were recorded in the 4000 to 400 cm⁻¹ range to characterize bond formation and functional groups of the synthesized materials. High-resolution transmission electron microscopy (HR-TEM) and selected area electron diffraction (SAED) patterns were used to investigate the texture and morphology of the cobalt ferrite nanoparticles. The HR-TEM and SAED analyses were performed using a JEOL JEM-2100 microscope operated at an acceleration voltage of 200 kV. For HR-TEM imaging, samples were prepared by depositing them on a carbon-coated copper grid followed by ultrasonic treatment for 15 minutes. Additionally, the morphology and energy-dispersive X-ray spectroscopy (EDS) data of the samples were obtained using a field emission scanning electron microscope (FE-SEM) Thermo Scientific Quattro S equipped with a field emission gun (FEG). UV-visible diffuse reflectance spectra of the samples were recorded over the 200–1200 nm range using a Jasco V-670 UV-vis spectrophotometer coupled with an integrating sphere.

RESULTS AND DISCUSSION

Synthesis and characterization of CoFe2O4 nanostructures

• Synthesis of CoFe₂O₄ nanostructures

Nanoparticles of cobalt ferrite (CoFe₂O₄) were produced by a simple, one-pot hydrothermal process. Inexpensive materials including ammonia solution, iron(III) nitrate nonahydrate, and cobalt(II) nitrate hexahydrate were hydrothermally treated for a brief period without further heat treatment in order to accomplish this. The hydrothermal treatment's end products were fine-tuned by investigating how several experimental factors, such as reaction duration, temperature, ethylene glycol (EG) concentration, pH value, and AG concentration, affected the hydrothermal processes. As we'll see in a little, X-ray diffraction (XRD) was the primary tool for studying the hydrothermal treatment optimization process. As a result of the optimization procedure, Table 1 displays the crystallite sizes (D_XRD) of the cobalt ferrite (CoFe₂O₄) products. Product characterization also made use of field emission scanning electron microscopy (FE-SEM), transmission electron microscopy (TEM), Fourier transform infrared spectroscopy (FT-IR), ultraviolet-visible spectroscopy (UV-vis), and diffuse reflectance spectroscopy (DRS), among other additional methods.

Table 1 Symbols and DXRD values of the hydrothermally prepared samples

Sample	Factor under study	DXRD (nm)	Sample	Factor under study	DXRD (nm)
CF-0.5	0.5 h	3.6	CF-EG25	25% EG	8.5
CF-4	4 h	7.8	CF-W	Water	12.9
CF-8	8 h	8.5	CF-W-9.6	3 M, 50 mL	12.9
CF-180	180 ∘C	7.8	CF-W-9	3 M, 36 mL	12.7
CF-150	150 ∘C	6.1	CF-W-8	3 M, 30 mL	12.3
CF-120	120 ∘C	4.5	CF-AG-0	Without AG	12.9
CF-EG100	100% EG	7.8	CF-AG-0.5	0.5 g AG	12.4
CF-EG75	75% EG	8.1	CF-AG-1	1 g AG	12.1
CF-EG50	50% EG	8.4	CF-AG-2	2 g AG	11.1



• Effect of reaction time

We looked at how the cobalt ferrite nanoparticle manufacturing method changed depending on the hydrothermal treatment reaction time. Figure 1 displays the X-ray diffraction (XRD) patterns of the products produced at different durations of hydrothermal treatment. At 20 values of 18.2° (111), 30.08° (220), 35.4° (311), 43.05° (400), 53.4° (422), 56.9° (511), 62.5° (440), and 74.01° (533), the hydrothermal treatment samples exhibit unique Bragg diffraction peaks. The cubic spinel structure of cobalt ferrite (CoFe₂O₄), space group Fd3m (227), and lattice parameters of a = b = c = 8.3 Å, $\alpha = \beta = \gamma = 90^{\circ}$ are all described by the peaks that match the database reference pattern JCPDS card no. 22-1086 (ref. 26). No peaks from other crystalline contaminants have been identified. The XRD reflection peaks of the products were made sharper and narrower by extending the hydrothermal reaction period from 0.5 hours to 8 hours, as shown in Figure 1.

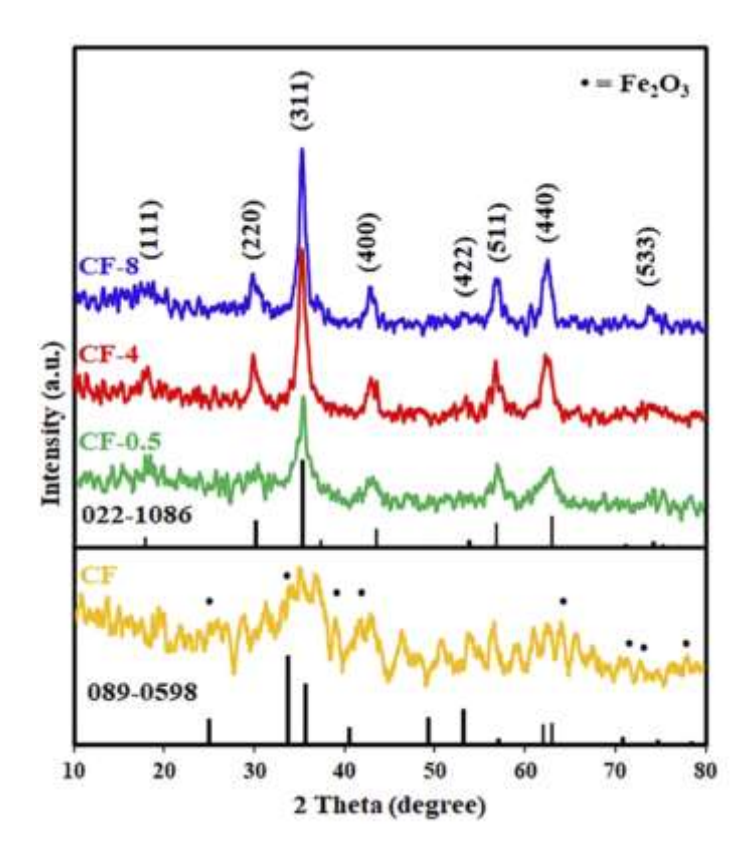


Figure 1: RD patterns of samples prepared by co-precipitation (CF) and hydrothermal methods at 0.5, 4, and 8 h $\,$

It follows that the products be more crystallinity the longer the hydrothermal reaction time is. In order to get an idea of the produced samples' typical crystallite sizes, the Debye-Scherrer formula was used (1).

$$D_{\rm XRD} = K \lambda / \beta \cos \theta \tag{1}$$

The equation includes the following variables: crystallite size (nm), a constant K linked to the crystal's form (= 0.89), b, the X-ray wavelength (λ = 1.5406 Å for Cu K α), and θ , Bragg's angle of diffraction. Results showed that CF-8 had the biggest average crystallite size at 8.5 nm and the CF-0.5 sample had the smallest at 3.6 nm. But because 4 hours produced a CF-4 product with high crystallinity, we have decided that this is the optimal hydrothermal reaction period. In addition to the fact that there is no discernible difference between CF-4 and CF-8, the 4-hour hydrothermal reaction time also conserved energy and time.

Ostwald ripening is responsible for the nucleation and development of cobalt ferrite (CoFe₂O₄) particles. The dissolution of small-sized particles and their subsequent redeposition into larger-sized particles is known as the Ostwald ripening process. This could happen because bigger particles are energetically unfavorable due to their lower surface energy and overall Gibbs energy compared to smaller particles. It is worth mentioning that our findings align with those previously documented in the literature. For example, it is likely because of the Ostwald ripening process that observed that the average size of the CoFe₂O₄ nanoparticles produced by the hydrothermal approach was marginally bigger than the average diameter of the particles produced by the conventional co-precipitation method. The researchers used hydrothermal Ostwald ripening to create hollow anatase TiO₂ nanospheres. They showed that the products' crystallinity rose steadily from 2 to 100 hours of reaction time. Increasing the reaction period from 2 to 6

hours improved the formation of crystallites of CoFe₂O₄ nanoparticles using the hydrothermal technique, according authors.

We used the standard co-precipitation technique at 70 °C to conduct the reaction of cobalt(II) nitrate hexahydrate and iron(III) nitrate nonahydrate with ammonium hydroxide in order to make a comparison. A semi-amorphous cubic cobalt ferrite (CF) with JCPDS card no. 22-1086 (ref. 26) and other phases, such as hematite with JCPDS card no. 89-0598, was formed by the co-precipitation procedure, but it did not yield pure cobalt ferrite nanoparticles, as seen in Figure 1. Recent studies have shown that hydrothermal procedures can yield the desired CoFe₂O₄ product in a single, easy step, eliminating the need for post-thermal treatment, in contrast to the co-precipitation method, which was unable to achieve a pure cobalt ferrite phase.

• Effect of temperature

A hydrothermal reaction of interest was examined to determine the effect of a reaction temperature ranging from 120 to 180 °C. In Fig. 2, you can see the goods' XRD patterns. Figure 2 shows that the crystallinity and purity of the products are significantly affected by the temperature of the hydrothermal process.

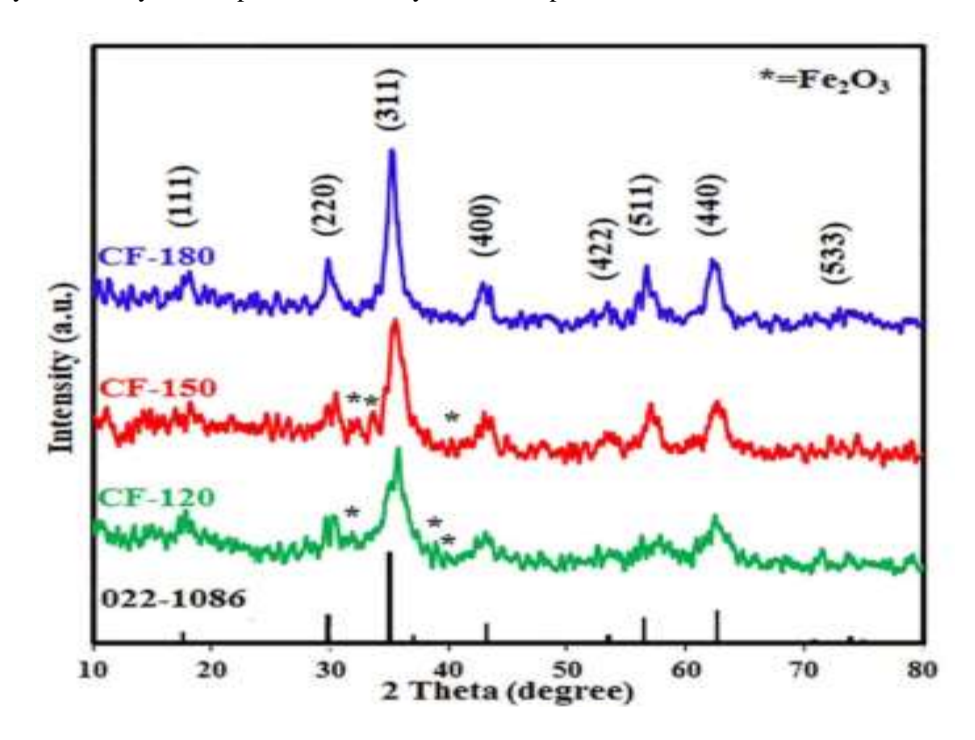


Figure 2: XRD patterns of hydrothermal products.

According to the findings, a pure cobalt ferrite product with an average crystallite size of 7.8 nm was formed at a reaction temperature of 180 °C, while reducing the temperature had a detrimental effect on the crystallinity and purity of the cobalt ferrite (CoFe₂O₄) product. At reduced reaction temperatures of 150 and 120 °C, respectively, CoFe₂O₄ products CF-150 and CF-120 were produced, along with other phases. The former had smaller crystallite sizes of 6.1 nm while the latter had 4.5 nm. One of the impurities was hematite, which was identified by the diffraction peaks at 2θ values of 31.9° (009), 33.9° (109), 38.8° (209), and 40.3° (316).

Consequently, for the following reactions, a reaction temperature of $180\,^{\circ}\text{C}$ was determined to be optimal for this hydrothermal treatment. Because the precursors may have been more reactive at higher temperatures and the lattice rearrangement was aided, the hydrothermally synthesized cobalt ferrite result is likely very pure. The results obtained align well with those reported by who discussed the synthesis of monodispersed iron manganese oxide (Mno.43Fe2.57O4) nanoparticles using [Fe2MnO(O2CtBu)6(HO2CtBu)3] as a single source precursor, and [Co4Fe2O2(O2CtBu)10(MeCN)2] as a bimetallic pivalate cluster of [Fe2CoO(O2CtBu)6(HO2CtBu)3] as a single source precursor, respectively.

• Effect of solvent

Additionally, we looked at how different solvents affected the hydrothermal production of cobalt ferrite ($CoFe_2O_4$) nanoparticles. We achieved this by conducting the hydrothermal reactions in a variety of solvents, including water (H_2O , W), ethylene glycol (EG), and combinations of the two (% EG (v/v)). Figure 3 displays the XRD patterns that were obtained. The XRD data showed that a decrease in the ethylene glycol ratio led to an increase in the intensity of the diffraction peaks.



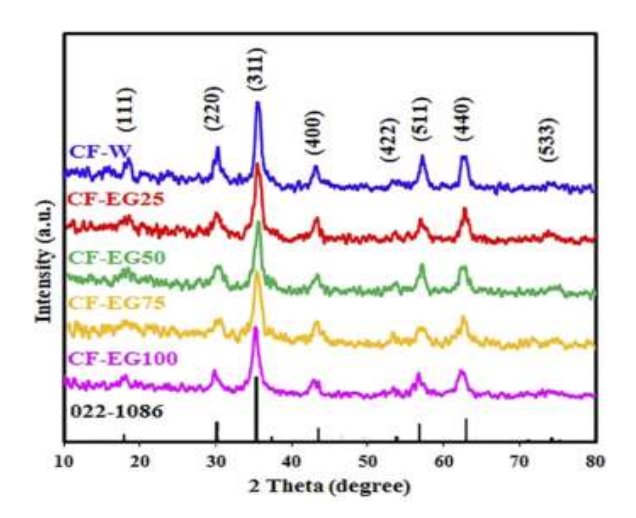


Figure 3: RD patterns of hydrothermal products

With 100% ethylene glycol (EG), the resultant crystallite size was 7.8 nm; with 100% water (H₂O), it rose to 12.9 nm. These findings suggest that the presence of ethylene glycol as a capping agent during the nuclei's formation may explain why the crystallinity of the cobalt ferrite (CoFe₂O₄) product decreased when 100% ethylene glycol was used as a pure solvent. Ethylene glycol may also limit growth rate and crystallite size creation by forming complexes with the metal ions of the metal precursors used. As an added bonus, water has a lower viscosity than ethylene glycol. Due to the increased ion mobility in water, bigger cobalt ferrite particles may form in aqueous conditions when the growth rate surpasses the nucleation rate. For all of these reasons—including the fact that it is the most cost-effective and ecofriendly solvent—we decided that water solvent would be best for our investigation.

Researcher also found findings that are consistent with these. Using ethylene glycol of several weight percentages, they studied how the surfactant affected the optical, structural, and magnetic characteristics of strontium ferrite (SrFe₂O₄) nanoparticles. Researchers found that the produced materials' crystallinity and diffraction peak intensity were both decreased when ethylene glycol weight percentages were increased. In addition, the results published by authors. and those investigated by authors. about the usage are consistent with one another. Using ethylene glycol of several weight percentages, they studied how the surfactant affected the optical, structural, and magnetic characteristics of SrFe₂O₄ nanoparticles. Researchers found that the produced materials' crystallinity and diffraction peak intensity were both decreased when ethylene glycol weight percentages were increased.

Authors looked at what happened when different glycols with different chain lengths (ethylene glycol (EG), diethylene glycol (DEG), and polyethylene glycol (PEG)) were used as solvents. By increasing the chain length of the ethylene glycol derivatives employed, the crystallite size for zinc ferrite (ZnFe₂O₄) products was reduced. They came to the conclusion that the structure of the intermediate complex may also be connected to the degree of crystallinity of the zinc ferrite products.

Effect of pH

A 3 M ammonia solution was added to the reaction medium in the appropriate amount to change its pH to 8, 9, and 9.6. Figure 4 shows the XRD patterns of the products.

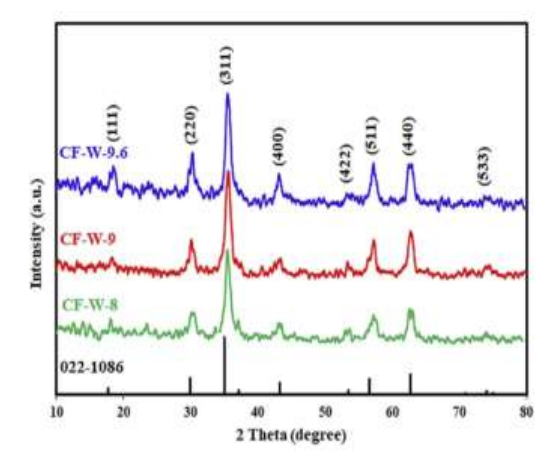
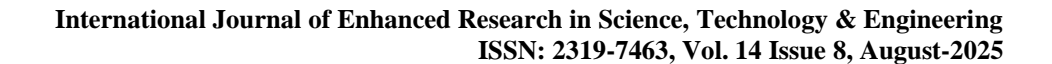


Figure 4: XRD patterns of hydrothermal products





As the pH value was raised, the products' crystallinity rose, according to the findings. A pH of 9.6 was determined to be optimal. The following also provides an explanation for these findings. Increasing the pH caused the precipitation of cobalt ions $[Co(H_2O)_6]^{2^+}$; the most abundant of these molecules may be $Co(OH)_x^{2^-x}$, which might undergo transformation into molecules with a lower solubility index $(Co(OH)_2)$. The precipitation point for cobalt ions is greater than that of iron ions because cobalt salt is more soluble than iron salt. The presence of the remaining cobalt was verified and identified by using a sodium hydroxide solution, which resulted in the production of a blue precipitate. The light pink hue of the supernatant after the hydrothermal reaction of the prepared samples at pH values of 8 and 9 was proof of this. The conclusion of the hydrothermal reaction was indicated by the colorlessness of the supernatant at a pH value of 9.6. Others also found similar outcomes.

Using the experimental design of CoFe₂O₄ nanoparticles generated by the EDTA/citrate complexing technique and the hydrothermal method, authors studied the impact of the pH factor on the crystallite size. It was suggested that the hydrolysis step, which is pH-dependent, might be associated with the improved crystallinity of the products. When there is an excess of sodium hydroxide, which results in a high pH, the cobalt hydroxide that forms is encased in several hydroxyl groups, causing the formation of large particles.

The authors found that increasing the pH value resulted in an increase in crystallinity of the obtained samples of $Co_{1-x}Zn_xFe_2O_4$ ($0 \le x \le 0.8$) nanoparticles synthesized using the microwave refluxing technique. The co-precipitation approach was used to manufacture 43 distinct pH-values of cobalt ferrite nanoparticles. Product XRD examination revealed that samples created at higher pH levels included only the $CoFe_2O_4$ phase, while samples prepared at lower pH levels contained both the $CoFe_2O_4$ and α -Fe₂O₃ phases.

Fourier transform infrared investigation (FT-IR)

As shown in Figure 5, Fourier transform infrared (FT-IR) spectroscopy was used to examine the hydrothermally produced products and determine their chemical composition and functional groups. Cobalt ferrite nanoparticles (CoFe₂O₄), a phase observed in all samples, were likely formed, as evidenced by two bands appearing in the FT-IR spectra around 416 cm⁻¹ and 590 cm⁻¹, corresponding to the vibrational frequencies of Co–O bonds in octahedral sites and Fe–O bonds in tetrahedral sites, respectively. Additionally, bands at approximately 3385 cm⁻¹ and 1616 cm⁻¹ correspond to the stretching vibration of O–H bonds and the bending vibration of H–O–H bonds, originating from moisture and Arabic gum residue, respectively. The broad band near 3385 cm⁻¹ is likely due to overlapping stretching vibrations of O–H and N–H bonds. Furthermore, vibrational bands at around 2925 cm⁻¹ and 2859 cm⁻¹, observed in Figure 5(e), can be attributed to the asymmetric and symmetric stretching vibrations of the CH₂ groups in the organic Arabic gum residue.

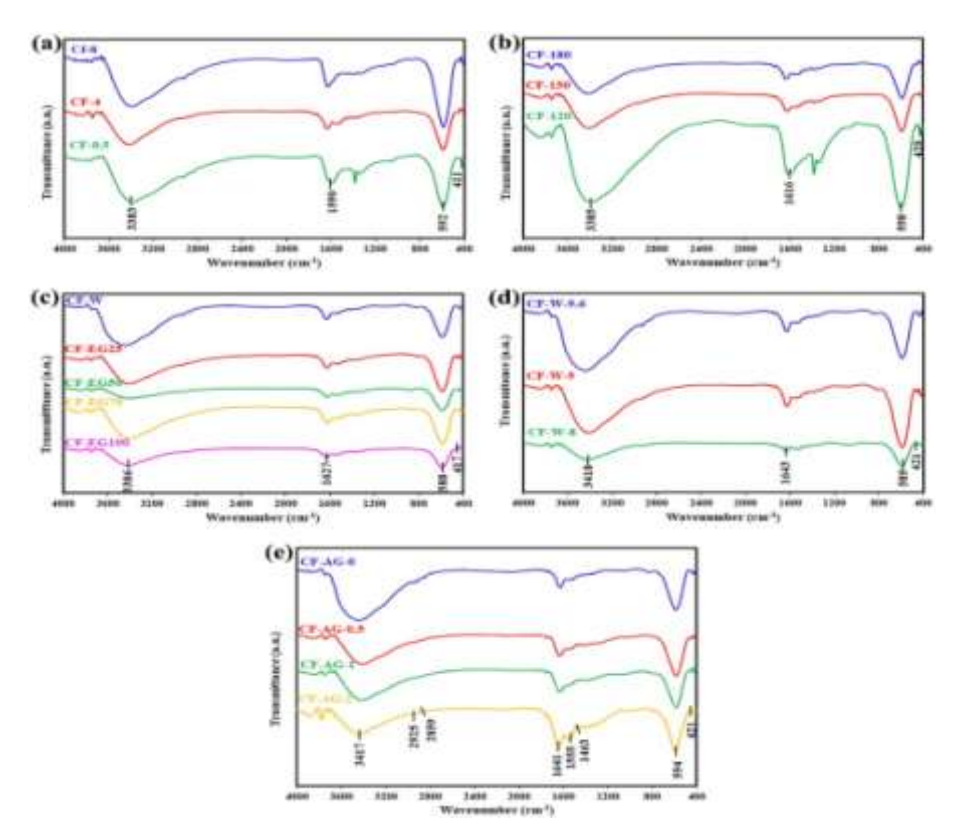


Figure 5: TIR spectra of hydrothermal samples varying in (a) time, (b) temperature, (c) solvent (water-EG ratios), (d) Ph and (e) Arabic gum amount



This figure also displayed the bending vibration of H–C–H at approximately 1463 cm⁻¹, the stretching vibration of C=O at around 1743 cm⁻¹, and the bands corresponding to the symmetric and asymmetric stretching vibrations of the COO⁻ groups at about 1555 cm⁻¹ and 1517 cm⁻¹, respectively. These bands are attributed to the excess Arabic gum used in the hydrothermal treatment.

The morphology

The morphological properties of cobalt ferrite nanoparticles (CoFe₂O₄ NPs) were investigated using field-emission scanning electron microscopy (FE-SEM), high-resolution transmission electron microscopy (HR-TEM), and selected area electron diffraction (SAED) techniques. Particle sizes of the CoFe₂O₄ NPs were determined from size distribution histograms. FE-SEM images of the samples CF-EG100, CF-EG50, CF-W, and CF-AG-0.5 at various magnifications are shown in Figure 6(a–h).

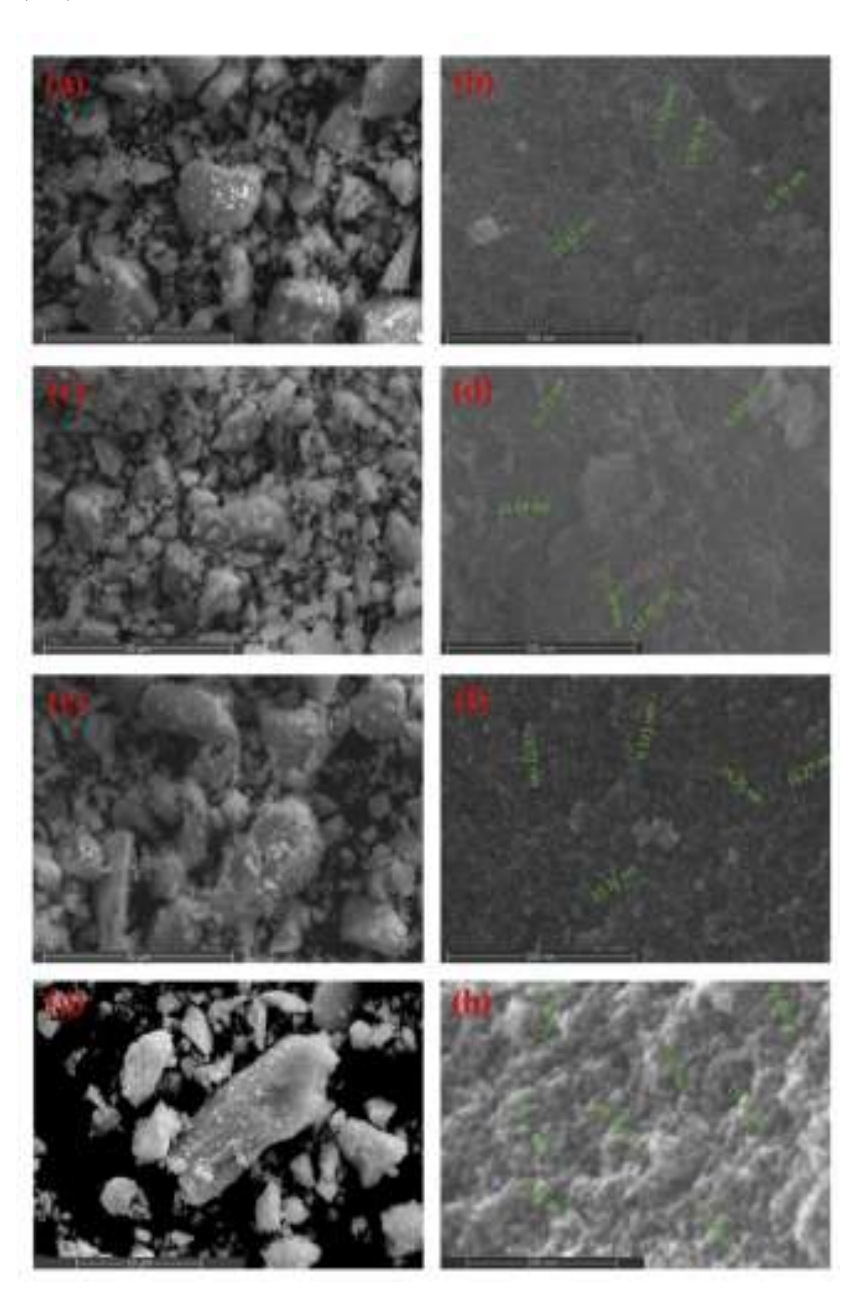


Figure 6: FE-SEM images of samples at different magnifications

Energy-dispersive X-ray spectroscopy (EDS) analysis

The samples CF-EG100, CF-W, and CF-AG-0.5 were analyzed by Energy-Dispersive X-ray Spectroscopy (EDS), as shown in Figure 7 (a-c). The data confirmed the successful synthesis of cobalt ferrite, as the samples contained only iron, cobalt, and oxygen, with trace amounts of carbon as impurities. The presence of carbon could be attributed to residues from ethylene glycol, Arabic gum, or contamination from organic pollutants during sample preparation for EDS analysis. The inset tables in Figure 7 display the Fe/Co molar ratios, which were 2.11, 1.93, and 2.14 for CF-EG100, CF-W, and CF-AG-0.5, respectively, consistent with the expected stoichiometric ratios.



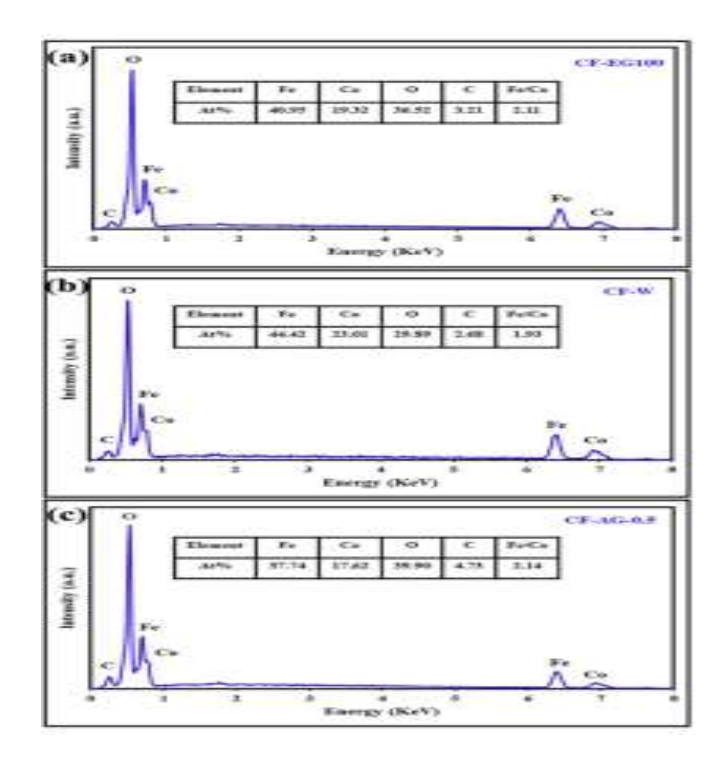


Figure 7: DS spectra of CF-EG100 (a), CF-W (b), and CF-AG-0.5 (c) samples

CONCLUSION

In this study, cobalt ferrite (CoFe₂O₄) nanoparticles were successfully synthesized using an eco-friendly hydrothermal method without any post-processing steps such as calcination. The use of ethylene glycol as a solvent and Arabic gum as a natural stabilizer provided a green and effective medium for the formation of well-defined nanoparticles. The hydrothermal synthesis route proved advantageous in controlling particle morphology, crystallinity, and dispersion, while maintaining low energy consumption and minimizing environmental impact. The optimization of various synthesis parameters—such as reaction time, temperature, pH, ethylene glycol concentration, and Arabic gum content—allowed for the fine-tuning of nanoparticle properties. Comprehensive characterization using XRD, FT-IR, HR-TEM, SAED, FE-SEM, EDS, and UV-Vis diffuse reflectance confirmed the successful formation of spinel-structured cobalt ferrite nanoparticles with good crystallinity and uniform morphology. The results highlighted the strong potential of this green synthesis route for producing cobalt ferrite suitable for applications in catalysis, magnetic storage, and biomedicine. Overall, the method presents a sustainable, cost-effective, and scalable approach to nanomaterial production, aligning with the principles of green chemistry and environmental responsibility. This work opens new avenues for the development of functional magnetic nanomaterials using clean synthesis techniques.

REFERENCES

- [1]. M. Weißpflog, N. Nguyen, N. Sobania, and B. Hankiewicz, "Non-Stoichiometric Cobalt Ferrite Nanoparticles by Green Hydrothermal Synthesis and their Potential for Hyperthermia Applications," *J. Phys. Chem. C*, vol. 128, no. 37, 2024, doi: 10.1021/acs.jpcc.4c03589.
- [2]. Q. Tamboli, S. M. Patange, Y. Mohanta, R. Sharma, and K. Zakde, "Green Synthesis of Cobalt Ferrite Nanoparticles: An Emerging Material for Environmental and Biomedical Applications," *J. Nanomater.*, vol. 2023, no. 8–9, pp. 1–15, 2023, doi: 10.1155/2023/9770212.
- [3]. P. Coppola, F. Gomes da Silva, G. Gomide, F. Paula, A. Campos, R. Perzynski, C. Kern, J. Depeyrot, and R. Aquino, "Hydrothermal synthesis of mixed zinc–cobalt ferrite nanoparticles: structural and magnetic properties," *J. Nanopart. Res.*, vol. 18, no. 5, 2016, doi: 10.1007/s11051-016-3430-1.
- [4]. Zalite, G. Heidemane, L. Kuznetsova, and M. Mairov, "Hydrothermal Synthesis of Cobalt Ferrite Nanosized Powders," *IOP Conf. Ser.: Mater. Sci. Eng.*, vol. 77, no. 1, 2015, doi: 10.1088/1757-899X/77/1/012011.
- [5]. Y. Koseoglu, F. Alan, M. Tan, R. Yilgin, and M. Öztürk, "Low Temperature Hydrothermal Synthesis and Characterization of Mn Doped Cobalt Ferrite Nanoparticles," *Ceram. Int.*, vol. 38, no. 5, pp. 3625–3634, 2012, doi: 10.1016/j.ceramint.2012.01.001.
- [6]. B. Aslibeiki, P. Kameli, H. Salamati, M. Eshraghi, and T. Tahmasebi, "Superspin glass state in MnFe₂O₄ nanoparticles," *J. Magn. Magn. Mater.*, vol. 322, no. 19, pp. 2929–2934, 2010.
- [7]. J. Jiang and L. H. Ai, "Synthesis and characterization of Fe-Co binary ferrospinel nanospheres via one-step nonaqueous solution pathway," *Mater. Lett.*, vol. 64, no. 8, pp. 945–947, 2010.
- [8]. M. G. Naseri, E. Saion, H. A. Ahangar, A. Shaari, and M. Hashim, "Simple Synthesis and Characterization of



- Cobalt Ferrite Nanoparticles by a Thermal Treatment Method," *J. Nanomater.*, vol. 2010, 2010, doi: 10.1155/2010/907686.
- [9]. L. Chen, Y. Shen, and J. Bai, "Large-scale synthesis of uniform spinel ferrite nanoparticles from hydrothermal decomposition of trinuclear heterometallic oxo-centered acetate clusters," *Mater. Lett.*, vol. 63, no. 12, pp. 1099– 1101, 2009.
- [10]. M. Gharagozlou, "Synthesis, characterization and influence of calcination temperature on magnetic properties of nanocrystalline spinel Co-ferrite prepared by polymeric precursor method," *J. Alloys Compd.*, vol. 486, no. 1–2, pp. 660–665, 2009.
- [11]. Z. Zi, Y. Sun, X. Zhu, Z. Yang, J. Dai, and W. Song, "Synthesis and magnetic properties of CoFe₂O₄ ferrite nanoparticles," *J. Magn. Magn. Mater.*, vol. 321, no. 9, pp. 1251–1255, 2009.
- [12]. H.-M. Fan, J.-B. Yi, Y. Yang *et al.*, "Single-crystalline MFe₂O₄ nanotubes/nanorings synthesized by thermal transformation process for biological applications," *ACS Nano*, vol. 3, no. 9, pp. 2798–2808, 2009.
- [13]. H. Gul and A. Maqsood, "Structural, magnetic and electrical properties of cobalt ferrites prepared by the sol-gel route," *J. Alloys Compd.*, vol. 465, no. 1–2, pp. 227–231, 2008.
- [14]. J. Zhang and C. Q. Lan, "Laser-generated Ni and Co nanoparticles in organic media," *Mater. Lett.*, vol. 62, no. 10–11, pp. 1521–1524, 2008.
- [15]. V. L. Calero-DdelC and C. Rinaldi, "Synthesis and magnetic characterization of cobalt-substituted ferrite (CoxFe₃-xO₄) nanoparticles," *J. Magn. Magn. Mater.*, vol. 314, no. 1, pp. 60–67, 2007.
- [16]. D. Zhao, X. Wu, H. Guan, and E. Han, "Study on supercritical hydrothermal synthesis of CoFe₂O₄ nanoparticles," *J. Supercrit. Fluids*, vol. 42, no. 2, pp. 226–233, 2007.
- [17]. G. Baldi, D. Bonacchi, C. Innocenti, G. Lorenzi, and C. Sangregorio, "Cobalt ferrite nanoparticles: the control of the particle size and surface state and their effects on magnetic properties," *J. Magn. Magn. Mater.*, vol. 311, no. 1, pp. 10–16, 2007.
- [18]. M. H. Khedr, A. A. Omar, and S. A. Abdel-Moaty, "Magnetic nanocomposites: preparation and characterization of Co-ferrite nanoparticles," *Colloids Surf. A*, vol. 281, no. 1–3, pp. 8–14, 2006.
- [19]. S. Singhal, J. Singh, S. K. Barthwal, and K. Chandra, "Preparation and characterization of nanosize nickel-substituted cobalt ferrites (Co₁–xNixFe₂O₄)," *J. Solid State Chem.*, vol. 178, no. 10, pp. 3183–3189, 2005.
- [20]. J. B. Silva, W. De Brito, and N. D. S. Mohallem, "Influence of heat treatment on cobalt ferrite ceramic powders," *Mater. Sci. Eng. B*, vol. 112, no. 2–3, pp. 182–187, 2004.
- [21]. Y. Sui, X. Huang, Z. Ma *et al.*, "The effect of thermal annealing on crystallization in a-Si:H/SiO₂ multilayers by using layer-by-layer plasma oxidation," *J. Phys. Condens. Matter*, vol. 15, no. 34, pp. 5793–5800, 2003.
- [22]. M. Sugimoto, "The past, present, and future of ferrites," J. Am. Ceram. Soc., vol. 82, no. 2, pp. 269–280, 1999.
- [23]. K. V. P. M. Shafi, A. Gedanken, R. Prozorov, and J. Balogh, "Sonochemical preparation and size-dependent properties of nanostructured CoFe₂O₄ particles," *Chem. Mater.*, vol. 10, no. 11, pp. 3445–3450, 1998.
- [24]. P. Alivisatos, "Semiconductor clusters, nanocrystals, and quantum dots," *Science*, vol. 271, no. 5251, pp. 933–937, 1996.
- [25]. V. Pillai and D. O. Shah, "Synthesis of high-coercivity cobalt ferrite particles using water-in-oil microemulsions," *J. Magn. Magn. Mater.*, vol. 163, no. 1–2, pp. 243–248, 1996.